Nanosystems based on siRNA silencing HuR expression counteract diabetic retinopathy in rat

Marialaura Amadio [1]*, Alessia Pascale [1]*, Sarha Cupri[§2], Rosario Pignatello[§2], Cecilia Osera[1], Velia D'Agata [3], Agata Grazia D'Amico [3], Gian Marco Leggio[3], Barbara Ruozi[4], Stefano Govoni [1], Filippo Drago[3], Claudio Bucolo[3§]

[1]Department of Drug Sciences, Section of Pharmacology, University of Pavia, Pavia, Italy; [2]NANO-i – Research Center on Ocular Nanotechnology – Department of Drug Sciences, University of Catania, Catania, Italy; [3]Department of Biomedical and Biotechnological Sciences, School of Medicine, University of Catania, Catania, Italy; [4] Nanomedicine Group, Te.Far.T.I. Center, Department of Life Sciences, University of Modena and Reggio Emilia, Modena, Italy.

* These two authors contributed equally to the work presented here and should therefore be regarded as equivalent authors.

§ corresponding author: Claudio Bucolo, Ph.D., FARVO, Department of Biomedical and Biotechnological Sciences, School of Medicine, University of Catania, Via S. Sofia 64, Catania, Italy. E-mail: claudio.bucolo@unict.it

Abstract

We evaluated whether specifically and directly targeting human antigen R (HuR), a member of embryonic lethal abnormal vision (ELAV) proteins family, may represent a new potential therapeutic strategy to manage diabetic retinopathy. Nanosystems loaded with siRNA silencing HuR expression (lipoplexes), consisting of solid lipid nanoparticles (SLN) and liposomes (SUV) were prepared. Photon correlation spectroscopy analysis, Zeta potential measurement and atomic force microscopy (AFM) studies were carried out to characterize the complexation of siRNA with the lipid nanocarriers. Nanosystems were evaluated by using AFM and scanning electron microscopy. The lipoplexes were injected into the eye of streptozotocin (STZ)-induced diabetic rats. Retinal HuR and VEGF levels were detected by Western blot and ELISA, respectively. Retinal histology was also carried out. The results demonstrated that retinal HuR and VEGF are significantly increased in STZ-rats and are blunted by HuR siRNA treatment. Lipoplexes with a weak positive surface charge and with a 4:1 N/P (cationic lipid nitrogen to siRNA phosphate) ratio exert a better transfection efficiency, significantly dumping retinal HuR and VEGF levels. In conclusion, we demonstrated that siRNA can be efficiently delivered into the rat retina using lipid-based nanocarriers, and some of the lipoplexes loaded with siRNA silencing HuR expression are potential candidates to manage retinal diseases.

Keywords: diabetic retinopathy; VEGF; HuR/ELAV; siRNA; solid lipid nanoparticles; liposomes

1. Introduction

Quality of life of diabetic patients elicited an enormous burden to the healthcare system in Western countries [1, 2]. Specifically, diabetic retinopathy (DR) represents a common complication of diabetes, still remaining one of the leading causes of blindness worldwide. DR, both non-proliferative and proliferative forms, is characterized by neuroretinal dysfunction and retinal vascular damage leading to visual impairment and, not rarely, blindness in aged individuals. DR involves early changes in the retina such as thickening of the basement membrane, capillary degeneration and alteration in the blood flow, and, among the various dysfunctions, it is characterized by an increase in the vascular endothelial growth factor (VEGF) signaling. Indeed, inhibition of VEGF-mediated pathological angiogenesis has been shown to improve vision in DR patients, although with various limitations [3, 4]. VEGF can be induced at transcriptional and/or post-transcriptional level by many factors, such as hypoxia, cytokines and oxidative stress. In particular, VEGF expression is regulated by RNA-binding proteins (RBPs), and among them a main role is played by the embryonic lethal abnormal vision (ELAV) proteins [5-7]. The ubiquitously expressed human antigen R (HuR; also called ELAVL1) represents one of the best characterized RBPs. HuR is involved in a variety of pathologies such as cancer, cardiovascular diseases, chronic inflammation and DR [8-13].

We recently demonstrated that, following diabetes-induction, HuR protein is up-regulated and it binds to the VEGF-encoding mRNA thus augmenting its protein expression, and contributing to abnormal increase of VEGF in the retina of diabetic rats [13]. These effects are blunted by the *in vivo* co-administration of a selective inhibitor of the protein kinase C β isoform (PKCβ), an upstream HuR activator [13]. In the present study, we aimed to evaluate whether specifically and directly targeting HuR may represent a new therapeutic strategy to hinder VEGF overexpression. To this purpose, in our DR animal model we tested the effects of intraocular administration of a small interfering RNA (siRNA) silencing HuR expression, by evaluating the protein expression of HuR itself, VEGF, and the retinal status of diabetic rats.

Since *in vivo* siRNA activity is often hampered by degradation before reaching the mRNA in the target tissue, nanotechnological approaches have been recently proposed to overcome this drawback. The nanocarriers for RNA presently investigated belong to the categories of viral or non-viral vectors. The former are naturally able to infect cells and transfer their genetic material into host cells; however, they possess some limitations linked to production difficulties and toxicity/immunogenicity. Non-viral vectors, such as cationic lipid-based nanocarriers, have thus been proposed with some success as an alternative. These vectors show no immune response and production scalability with acceptable costs [1, 2, 8].

In this study we loaded solid lipid nanoparticles (SLN) and liposomes loaded with siRNA silencing HuR expression, to assess their pharmacological profiles in a DR model.

2. Materials and Methods

2.1 Chemicals

Didecylmethylamonium bromide (DDAB) and ([(2,3-dioleoxy propyl]N,N,trimethylamoniomethylphosphate) (DOTAP), cholesterol (CHOL) polysorbate 80 (Tween® 80) and glucose were purchased from Sigma Aldrich (Milan, Italy); 1,2-dioleoyl-*sn*-glycero-3-phosphoethanolamine (DOPE) and 1,2-dipalmitoyl-*sn*-glycero-3-phosphatidylcholine (DPPC) were purchased from Echelon Biosciences Inc. (Salt Lake City, UT, USA). Softisan® 100, a mixture of triglycerides of saturated C10-C18 fatty acids, was gifted by IOI Oleo GmBH (Hamburg, Germany). The used Rn_Elavl 1_predicted_1 siRNA (Gene symbol: Elavl 1; Gene ID: 363854; target sequence 5'-CGGCTTGAGGCTTCAGTCCAA-3'; sense strand 5'GCUUGAGGCUUCAGUCCAATT-3'; antisense strand 5'-UUGGACUGAAGCCUCAAGCCG-3') was purchased from Qiagen (Milan, Italy) in 20-nmol FlexiTubes. All solvents were analytical grade commercial products and were used as received. RNAse-free water was purchased from Qiagen. HuR siRNA were obtained from ThermoFisher Scientific (Milan, Italy).

2.2. Preparation of nanocarriers

Liposomes were prepared by a combination of the thin layer evaporation technique and extrusion through polycarbonate membranes. An initial phospholipid film was produced with the following molar ratios: DOPE:Chol:DOTAP:DPPC = 4:2:2:2 (coded as Lipo-A; Table 1) or DOPE:Chol:DOTAP:DPPC = 4:2:4:2 (coded as Lipo-B; Table 1). The lipids were weighed in a glass test tube and solubilized in a mixture of chloroform/methanol (4:1, v/v); the solution was evaporated off under a nitrogen stream to remove the organic solvents, leading to a phospholipid film on the bottom of the tube. Each sample was left under *vacuum* in a Büchi oven at 30° C for 4-6 hours to eliminate any residual trace of the solvents. The phospholipid film was then hydrated with a solution of glucose (5%, w/v) prepared with RNAse free water [15]. The hydration was done by placing the vial in a water bath (46 ± 1 °C for 2 minutes), followed by vortexing for 2 minutes at room temperature. The entire process was repeated for three times, producing multilamellar vesicles (MLV). After an annealing step for 1 hour at room temperature, the MLV were extruded using a Liposofast® apparatus (Avestin, Canada). A first extrusion for 21 times with 400-nm pore polycarbonate membranes was followed by an analogous extrusion with 100-nm pore membranes, to get small unilamellar liposomes (SUVet) [15]. The preparation method used to obtain SLN (coded

as Lipo-C; Table 1) was a modification of the technique known as Quasi-Emulsion Solvent Diffusion (QESD) [16, 17]. An organic phase (2 ml) consisting of Softisan® 100 (0.60% w/v) and DDAB (0.03%, w/v) in acetone was added dropwise through a thin teflon tube connected to an insulin syringe into a 25-ml glass tube containing the aqueous phase (0.05% w/v Tween® 80 in 10 ml water), kept at 0°C in an ice bath, under stirring at 24000 rpm by a UltraTurrax® T25, equipped with a G8 dispersing accessory (IKA GmbH, Königswinter, Germany), for 15 min. The obtained dispersion was sonicated for 4 minutes in an ice bath by a probe sonicator (Branson Sonifier 450, USA) at speed 6.All the nanocarriers used in the present study are nontoxic (data not shown).

2.3. Preparation of siRNA-carrier complexes

After a systematic study to determine the variables for carriers preparation (data not shown), selected carriers were used for the preparation of the siRNA-loaded lipoplexes, using various molar ratios of cationic lipid nitrogen (N) to siRNA phosphate (P) (N/P ratio). The N/P (+/−) ratio is an indicator of the ionic balance of the complexes: it refers to the number of residual nitrogen atoms of the cationic lipids compared to the phosphate groups of the siRNA. The N/P ratio was calculated by the following equation (considering 42 phosphate groups for each siRNA molecule):

$$\text{N/P ratio} = \frac{[+]}{[-]} = \frac{[\,Ammonium\ groups\ from\ cationic\ lipid]}{[Phophate\ groups\ from\ siRNA]}$$

The nanocarriers (SUVet and SLN) were sterilized by filtration through sterile 0. μm polyethersulfone filters (VWR International PBI, Milan, Italy) and incubated for 30 min with a solution of the lyophilized siRNA in RNAse-free water, at the established N/P ratio [15]. All steps were carried out under aseptic conditions. The complexation data are reported in Table 1.

2.4. Nanocarriers characterization

2.4.1 Photon Correlation Spectroscopy

The formed lipid carrier-siRNA complexes (lipoplexes) were analyzed by a Zetasizer Nano ZS90 (Malvern Instruments, UK) to determine the average particle size (Z-Ave) and the polidispersity index (PDI). Samples were diluted ten-fold with HPLC-grade water to avoid multiscattering phenomena, and analyzed in triplicate. The reported values are the mean ± SD of 90 measurements (three sets of 10 measurements in triplicate). The electrophoretic mobility and Zeta potential (ZP) were determined by Laser Doppler micro-electrophoresis using the same instrument. The apparatus consisted of a He-Ne laser with a maximal power of 4 mW, at a wavelength of 633 nm. Each sample was diluted 1:10 with HPLC-grade water. Up to 100 measurements on each sample were taken at 25°C with a measurement angle of 173° by disposable cuvettes to calculate the electrophoretic

mobility and, using the Smoluchowski constant f(Ka) with a value of 1.50, the corresponding ZP values.

2.4.2. Microscopy study

Liposome, SLN and the respective lipid carrier-siRNA complexes (lipoplexes) were evaluated by using atomic force microscopy (AFM) and scanning transmission electron microscopy (STEM). The AFM observations were performed with an Atomic Force Microscope (Park Instruments, Sunnyvale, CA, USA) at room temperature (about 20–25◦C) operating in air and in non-contact mode using a commercial silicon tip-cantilever (high resolution noncontact "GOLDEN" Silicon Cantilevers NSG-11, NT-MDT, tip diameter of about 5–10 nm; Zelenograd, Moscow, Russia) with stiffness about 40 Nm^{-1} and a resonance frequency around 170 kHz. A drop of each sample was diluted with distilled water (about 1:10 v/v) before to be applied on a small mica disk (1 cm × 1 cm); after 2 min, the excess of water was removed using paper filter, then the sample was analyzed. The AFM images were obtained with a scan rate of 1 Hz and processed using a ProScan Data Acquisition software. For STEM analysis, a drop of a water-diluted suspension of the samples (1:10 v/v) was placed on a 200-mesh formvar copper grid (TABB Laboratories Equipment, Berks, UK), allowed to adsorb and the surplus was removed by filter paper. Samples were then dried at room conditions and imaged with a Nova NanoSEM 450 (FEI Company, Hillsboro, Oregon, USA) operating in TEM mode (STEM detector) at an acceleration voltage of 30 KV..

2.5. Animal treatment

Male Sprague–Dawley rats weighing approximately 200 g were obtained from Envigo (Udine, Italy). All the animals were treated according to the EU Directive 2010/63/EU for animal experiments, and to the ARVO (Association for Research in Vision and Ophthalmology) Statement for the Use of Animals in Ophthalmic and Vision Research. The animals were fed on standard laboratory food and were allowed free access to water in an air-conditioned room with a 12-hours light/12-hours dark cycle. Induction of diabetes was obtained by streptozotocin (STZ, purchased from Sigma–Aldrich, Milan, Italy) as previously described [13, 14]. STZ destroys pancreatic island β cells and is used to induce experimental diabetes in rodents [18]. Adult rats treated with a single dose of STZ exhibit hyperglycemia within 48 hours, and these animals are widely used as a model of insulin-dependent diabetes. Control (CTR) animals received citrate buffer alone. After 24 hours, animals with blood

glucose levels >250 mg/dl were considered diabetic, and randomly divided into groups of ten animals each. The diabetic state was confirmed by daily evaluating glycaemia through a blood glucose meter. No supplemental insulin was administered to prevent weight loss. Ten days after STZ treatment, a naked HuR siRNA (2 µl in RNAse-free water; Qiagen, Milan, Italy) was intraocular administered and the animals (CTR, STZ, CTR+siRNA; STZ+siRNA) sacrificed 48 hours after siRNA injection. For the experiments with HuR siRNA delivered by nanocarriers, another group of diabetic animals was divided into subgroups treated with the vehicle or one of the nanocarriers carrying siRNA (lipoplex L1, L2, L3, and L4, respectively). Euthanasia was performed with CO_2 inhalation after 48 hours and the retina collected. Final group sizes for all measurements were n = 6–10 except as noted. As previously noted scrambled siRNA do not have any effect (data not shown).

2.6. Retinal HuR and VEGF measurement

Retinal tissues were homogenized in RIPA buffer (50 mM Tris-HCl, 150 mM NaCl, 1 mM EDTA, 0.25% Na-deoxycholate, 1% Nonidet, and a protease inhibitor cocktail) in a glass-teflon homogenizer, sonicated (10 sec for 2 times), and centrifuged (980 x g for 3 min at 4°C). The pellet was discarded; the protein content in the surnatant was measured according to Bradford's method using bovine albumin as a standard. Proteins of interest were analyzed by Western blotting or ELISA following standard procedures. For Western blotting, the anti-HuR mouse monoclonal antibody and the anti-α-tubulin rat monoclonal antibody (both from Santa Cruz Biotechnology, Santa Cruz, CA, USA) were diluted at 1:1000 in TBST buffer [10 mM Tris-HCl, 100 mM NaCl, 0.1% (v/v) Tween 20, pH 7.5] containing 6% milk. The nitrocellulose membranes were processed using Pierce ECL Plus from Thermo Scientific (Rockford, IL, USA). α-tubulin was used as housekeeping to normalize HuR data. Densitometric analysis was performed using the NIH Image software (http://rsb.info.nih.gov/nih-image). VEGF protein level was measured via an ELISA kit (R&D Systems Inc., Minneapolis, MN, USA) recognizing VEGF-A isoforms of 120, 164, and 188 amino acids, according to our previous publication [13]. Masked evaluation of HuR and VEGF levels was performed.

2.7. Retinal histology

Eyes were enucleated and fixed overnight with 4% paraformaldehyde in 0.1 M sodium phosphate (pH 7.6). The paraffin-embedded retina sections (5µm) were stained with hematoxylin–eosin, and the micrographs were photographed at 40× magnification under a light microscope (Axiovert, Carl Zeiss Inc) equipped with a digital colour camera [19]. The thicknesses of the total retina, inner plexiform layer (IPL), inner nuclear layer (INL) and outer retinal layers (ORL), including both outer plexiform

(OPL) and outer nuclear layers (ONL), were measured at 0.5 mm dorsally and ventrally from the optic disc. The number of retinal ganglion cells (RGCs) was calculated using the linear cell density (cells per 100 μm). Two measurements at adjacent locations in each hemisphere were performed, and the average of six measurements of three eyes was recorded as the representative value for each group.

2.8. Statistical analysis

All the experiments were repeated at least three times. For statistical analysis the GraphPad Instat statistical package (version 3.05 GraphPad software, San Diego, CA, USA) was used. The data were analyzed by analysis of variance (ANOVA) followed, when significant, by a specific *post-hoc* test, as indicated in the figure legends. Differences were considered statistically significant when p values < 0.05.

3. Results

3.1. Physico-chemical characterization of nanocarriers

In Table 1, the mean particle size and ZP values relative to the naked carriers and their siRNA complexes, produced at a 4:1 N/P ratio, are gathered. Lipo-A and Lipo-B unloaded SUVet appeared as homogeneous populations with a mean size close to 100 nm strictly related to the pore size of the extrusion membranes. The two liposomal systems only differ for the amount of cationic lipid (DOTAP) present in the bilayers; such a difference was reflected by their ZP, with the Lipo-B system that showed a more pronounced positive ZP than the Lipo-A one (Table 1). The SLN batch (Lipo-C) contained a unimodal population of nanoparticles with a mean size of 214 nm, thus suitable for ocular application, and a net positive ZP value due to the presence of the cationic lipid DDAB. For the complexation, the HuR siRNA molecules were bound to the surface of the cationic lipid vesicles through electrostatic interactions. This arrangement was highlighted by the relative increase in size (Z-Ave values) of the complexes compared to the unloaded (blank) carriers. The microscopic structure of lipoplexes was investigated by STEM and AFM microscopies, showing the presence of aggregates in Lipo-A siRNA. STEM images (Fig. 1) well identified the architecture of liposomes (Lipo-A), featured by a homogeneous contrast in which the double layer was well detectable with a decreased electron transparency in comparison with the core area, as described in a previous report [20]. Besides, liposomes seem to aggregate forming more complicated structures in which the siRNA is not detectable. The re-organization around the siRNA was confirmed by high resolution atomic force microscopy analyses in which siRNA strands are clearly detectable as partially surrounded by

lipidic material which looks like liposomes fused into assemblies (Fig. 1). STEM images showed Lipo-C siRNA complexes as complicated structures. In contrast with liposomal complexes (Lipo-A), the SLN siRNA complexes (Lipo-C) created structures characterized by a predominant and diffused electron dense area, surrounding siRNAs filaments and partially hiding the architecture of complexes. These structures showed irregular shape if compared with SLN alone (Lipo-C) indicated by the arrows (Fig. 1). AFM images confirm this hypothesis (Fig. 1). The observation that complexation of siRNA and cationic SUVet and SLN, respectively, did not deeply alter the size values and distribution of the lipoplexes compared to the native carriers is a proof that the adsorption of the oligonucleotide on the surface of preformed nanocarriers occurred in a well-organized and reproducible way, with no particle aggregation and significant increases in mean particle size. PDI values remained around or below 0.3, except for Lipo-A1 complex (Table 1), confirming the presence of homogeneous colloidal populations. Changes in ZP values were a further proof of the complexes generation through electrostatic interactions. A shift towards less positive or negative values was always recorded, caused by the ability of the negatively charged siRNA to shield the net positive charge of the lipid nanocarriers. The binding of siRNA with the cationic carriers was evaluated by measuring the ZP of complexes produced at different N/P ratios (Fig. 2). It was found that, by increasing the overall amount of cationic lipid, there is an increase of ZP ranging from -13.3 mV for naked siRNA, up to + 62 mV. These results confirm the good capacity of the cationic nanocarriers to neutralize the anionic charge of siRNA, forming complexes by electrostatic interaction. To evaluate the ability to block the expression of HuR protein *in vivo*, complexes between cationic SLN/liposome-RNA obtained at 4:1 (L1, L3, L4) and 10:1 (L2) N/P ratio were chosen. The complexation relationship (N/P ratio) also turned out to be decisive for the transfection efficiency (as shown later). The L2 complex, with a N/P ratio of 10:1, showed a lower mean diameter (~370 nm) and a more positive ZP value (+32.2 mV) compared to the corresponding lipoplex produced by a 4:1 N/P ratio (L1) (346 nm and +12.9 mV, respectively) (Table 1). Interestingly, at 20:1 N/P ratio all the three tested lipoplexes showed an almost identical ZP value (around +40 mV) (Fig. 2), suggesting that a similar degree of association of the siRNA molecules with the nanocarriers was reached. Conversely, above this N/P ratio the measured ZP values were close to those given by the unloaded carriers, indicating that a siRNA/lipid ratio below 1:40 gave a very low association efficiency on the surface of the liposomes and SLN.

3.2. Retinal levels of HuR and VEGF

A preliminary dose-ranging study (0.25, 2.5, 25 and 250 μM of siRNA) was carried out in STZ-induced diabetic rats in order to select the right dose of siRNA. HuR protein level was measured 48

hours after siRNA intraocular administration and, among the tested doses, 2.5μM HuR siRNA showed the most consistent decrease of retinal HuR in diabetic rats (mean expressed as percentage ± S.E.M.: STZ 100 % ± 7.38; STZ + siRNA 69.82 % ± 7.74; $p<0.05$; n=4-6). We then performed the treatment with 2.5 μM HuR siRNA in a larger group of animals, both control and diabetic, finding that HuR siRNA injected in STZ-rats restored HuR protein to control level in the retina, as shown in Fig. 3A. No significant changes of HuR level occur in control animals treated with siRNA. It is noteworthy that HuR siRNA is also able to reduce, without abolishing, VEGF levels in the retina of STZ-animals and to reinstate normal VEGF content (Fig. 3B).

Analogously, we tested the different nanocarriers loaded with 2.5 μM HuR siRNA, finding that the intraocular injection of either liposomes (L1 and L3) or SLN L4 significantly reduced both HuR and VEGF protein content in the retina of diabetic rats (Fig. 3). No changes were observed in STZ rats treated with lipoplex L2 (Fig. 3).

3.3 Histology

Diabetic rats showed a significant reduction in retina thickness, following the decrease of RGCs number (Fig. 4); this is consistent with previous studies [21, 22]. The treatment of diabetic rats with lipid-based nanocarriers complexed with siRNA reduced the retinal damage elicited by STZ, particularly with L1 system (Fig. 4). Intraocular administration of lipoplex L1 protects significantly ($p<0.05$) the retina maintaining the thickness to values (128.5 ± 0.4 μm) similar to those of control animals (130.6 ± 0.3 μm) and preserving the number of RGCs (12.5 ± 1.5 μm L1-treated group *vs.* 9.2 ± 1.0 μm STZ group; $p<0.05$). Lipoplexes L3 and L4 showed some retinal protection in terms of thickness and RGCs number, even though the effect was not statistically significant (data not shown); liposomal L2 complex did not show any retinal protection from STZ insult (data not shown), this latter result might be due to the different physico-chemical characteristics of these nanocarriers. The group treated with naked siRNA showed no retinal protection in terms of morphology (data not shown) after intravitreal injection. This finding could be explained by the lack of diffusion of the naked siRNA into the retinal layers or by the degradation from nucleases.

4. Discussion

We recently demonstrated [13] that the activation of the PKCβ/HuR/VEGF pathway at retinal level is implicated in diabetic retinopathy and HuR plays a key role in this disease. In general, ELAV proteins can form messenger ribonucleoprotein (mRNP) complexes that associate with the cytoskeleton and that, in turn, are linked to polysomes constituting a translational apparatus [23, 24]. It is well known that cytoskeleton represents an active site for protein synthesis [25] and mRNP complexes are committed to drive mRNAs to the translational machinery. In particular, we previously demonstrated [26] that HuR protein can target VEGF mRNA within mRNP complexes to the cytoskeleton, acting as a shuttle/chaperon protein. We in fact demonstrated the existence, in retinal pericytes, of a novel molecular pathway implicated in the government of VEGF gene expression at post-transcriptional level [26, 27]. We also showed that PKCβ is able to activate HuR protein that binds VEGF mRNA, within mRNP complexes, increasing VEGF protein content [26]. These previous studies thus opened the way to a novel pharmacological approach to counteract pathologies involving VEGF modification and to potentially manage the early phase of DR: by silencing HuR, the positive regulator of VEGF expression.

Several potential siRNA candidates are currently undergoing clinical trials such as bevasiranib, the first naked siRNA-based drug in clinical trials, which targets VEGF mRNA pathway for treatment of age-related macular degeneration and diabetic macular edema [28]. As therapeutic strategy, siRNA molecules offer several advantages over small-molecule drugs since the former can be easily designed and are characterized by high efficacy and specificity [29]; however the challenges are represented by their stability and delivery. In particular, delivery to the retina is challenging because of its anatomical and physiological complexities. A good example of retina complexity is the presence of the inner and outer blood–retina barriers, that are formed by tight junctions between adjacent endothelial cells, or between retinal pigment epithelial cells, respectively. Despite intravitreal administration having demonstrated notable superiority over other routes in enhancing retinal drug availability, there still exist various key points preventing optimal drug delivery into the retina. Even though siRNA is injected intraocularly, the stability and the sustained delivery to the target tissue represent the most challenging endeavors facing the pharmaceutical scientist. Intravitreal injection is the most direct approach for delivering drugs to the retina, and it is currently used in clinical practice for treatment with anti-VEGF drugs. Multiple injections are usually required increasing the risk of serious side effects such as infections and retinal detachment. Controlled and sustained delivery of ophthalmic drugs administered intravitreally represents a crucial point in order to decrease the number of injections, particularly for drugs with a short biological half-life such as naked siRNAs. The major goal of clinical therapeutics is to provide and maintain effective levels of drugs at the target tissue for an adequate time. To address the above points we prepared novel ocular formulations using SLN and

liposomes loaded with siRNA silencing HuR expression. After intravitreal administration, molecules encounter relatively fewer barriers in comparison with topical ocular route or systemic administration. Intravitreal route represents an important issue in terms of retinal siRNA delivery, with an impact as regards required dose, frequency and dosing intervals. However, major challenges are the lack of diffusion of therapeutic molecules throughout the retinal layers and the stability of siRNA towards degrading nucleases. Surprisingly, in our histological study, we observed that the group treated with naked siRNA showed no significant retinal protection in terms of morphology after intravitreal injection. This finding is probably due to the lack of diffusion of naked siRNA into the retinal layers or by the degradation from nucleases. Although naked siRNA was able to silence HuR and counteract VEGF, it was not able to protect the retina, likely due to its fast degradation. In the case of siRNAs, the production of nanocarriers represents a valid approach to improve retinal penetration and ameliorate stability. Treatment with lipoplexes L1, L3 and L4 significantly reduced HuR and VEGF compared to the STZ-group (Fig. 1, panels A and B). No effect was observed with liposomes L2 in terms of HuR and VEGF levels. This result could be related to the different N/P ratio (10:1 for L2 and 4:1 for L1, L3, and L4), suggesting that a higher N/P ratio contributes to reduce the cell transfection efficiency. These findings confirm a mechanism taking place at post-transcriptional level for HuR-mediated regulation of VEGF expression. The liposome binding to cells was linked to the residual positive charge of lipoplexes. Analyzing the *in vivo* findings of the SLN-based lipoplex L4 with the liposomes produced with the same N/P ratio (L1 and L3), a similar reduction of HuR and VEGF levels was observed (Fig. 2). The two liposomal complexes showed superimposable results, despite their difference in composition. Although Lipo-A and Lipo-C complexes shared a similar size (Table 1), SLN possesses a completely different matrix structure from the liposomal bilayers. Furthermore, the resulting lipoplex L4 displayed a negative ZP value, opposite to the corresponding vesicular lipoplexes L1 and L3. Such negative charge could explain the capability of siRNA molecules to uniformly cover the surface of the lipid matrix, as indicated by AFM and STEM analyses; in any case, this residual charge seems to affect the ability of the lipoplex L4 to interact with the target cells and induce their transfection, compared to the liposomal complexes bearing the same drug siRNA payload. In conclusion, in the present work we showed that lipoplexes loaded with siRNA silencing HuR expression represent potential candidates to manage retinal diseases such as DR.

Acknowledgements

This work was supported in part by the National grant PRIN 2009- BM7LJC.

Table 1. Mean size, size homogeneity (PDI) and surface charge of liposomes (Lipo-A and Lipo-B), SLN (Lipo-C) and their complexes with siRNA. Values represent the mean ± S.D. of three replicates.

Batch	N/P Ratio	Z-Ave (nm ± SD)	PDI ± SD	Zeta Potential (mV± SD)
Lipo-A	-	119.7 ± 1.908	0.069 ± 0.048	+54.4 ± 0.777
Lipo-A1 complex (L1)	4/1	346.1 ± 6.010	0.611 ± 0.033	+12.9 ± 0.665
Lipo-A2 complex (L2)	10/1	373.8 ± 35.820	0.314 ± 0.016	+32.2 ± 2.040
Lipo-B	-	116.0 ± 0.900	0.089 ± 0.026	+62.9 ± 0.651
Lipo-B complex (L3)	4/1	477.6 ± 4.424	0.305 ± 0.026	+15.7 ± 0.976
Lipo-C	-	214.0 ± 3.745	0.177 ± 0.014	+44.9 ± 8.840
Lipo-C complex (L4)	4/1	341.7 ± 7.480	0.240 ± 0.018	-9.36 ± 0.737

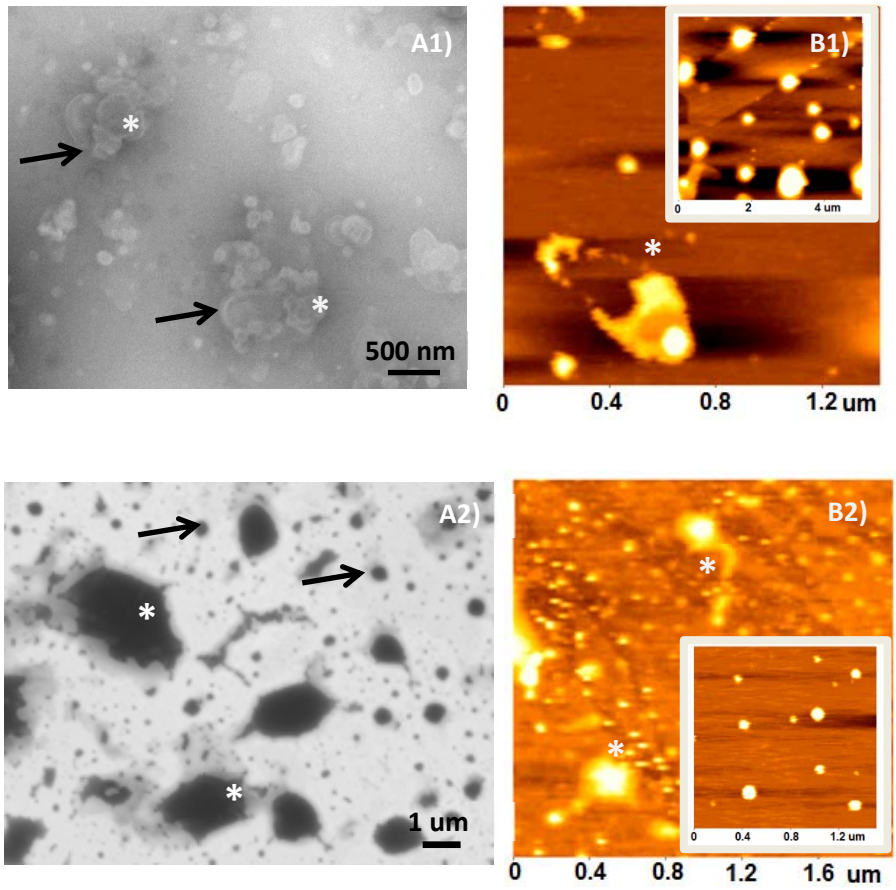

Fig. 1. Atomic force microscopy (AFM) and scanning transmission electron microscopy (STEM) of complexes: STEM (A) and AFM (B) images of Lipo-A siRNA complexes (1) and Lipo-C siRNA complexes (2). Arrows in A1 indicate the bilayer of liposomes while in A2 indicate the SLNs. Complexes are highlighted as *. AFM images of Lipo-A and Lipo-C are shown in the boxes inside panels B.

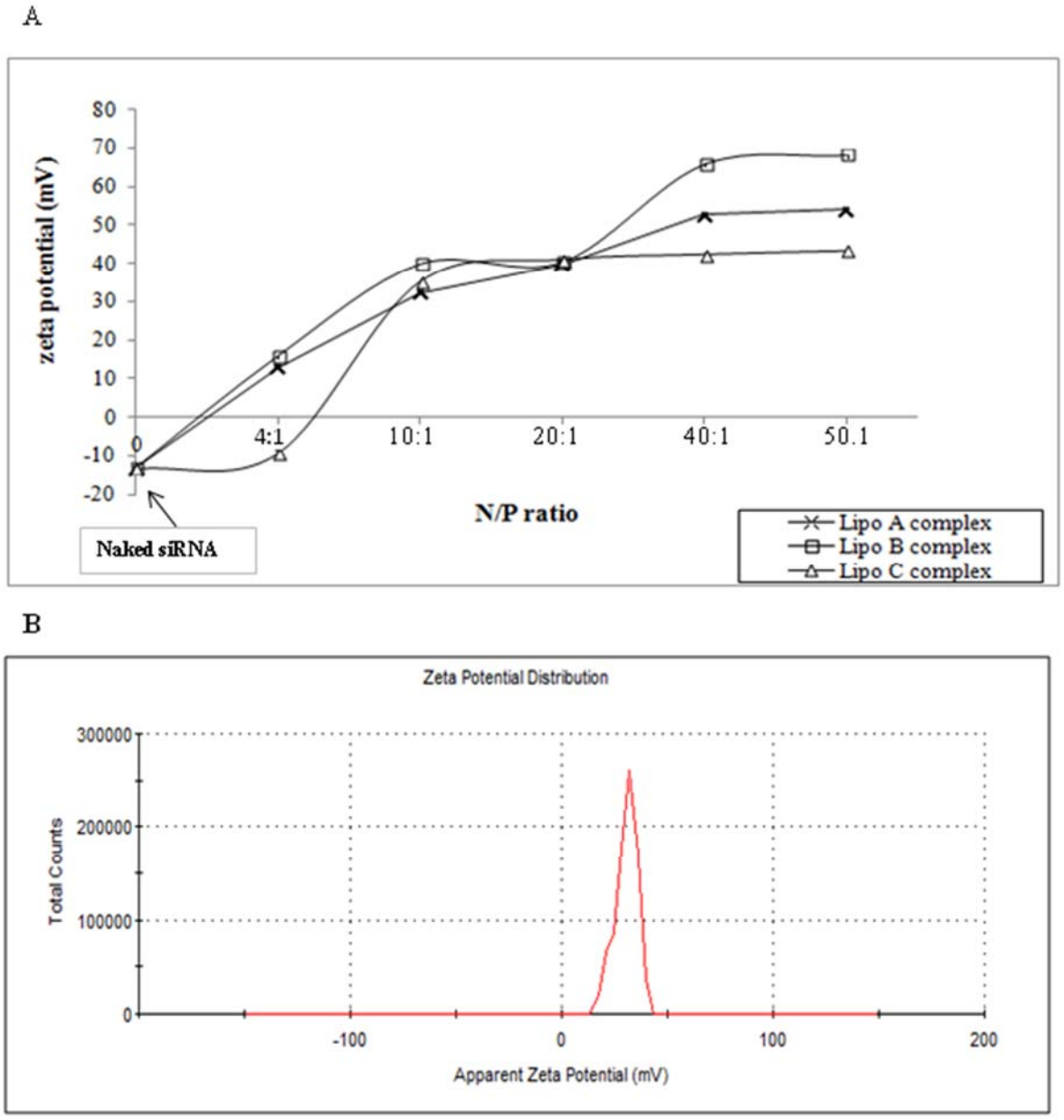

Fig. 2. A) Zeta Potential (ZP) values of RNA complexes with cationic liposomes (Lipo-A and Lipo-B) or SLN (Lipo-C) produced at different N/P ratios, measured in RNAse-free water after 30 min of incubation. Values are the mean ± S.D. of three determinations. Full symbols on the left side correspond to the ZP of unloaded (blank) lipocarriers; B) example of ZP analysis of the Lipo-A2 complex (10:1 N/P ratio).

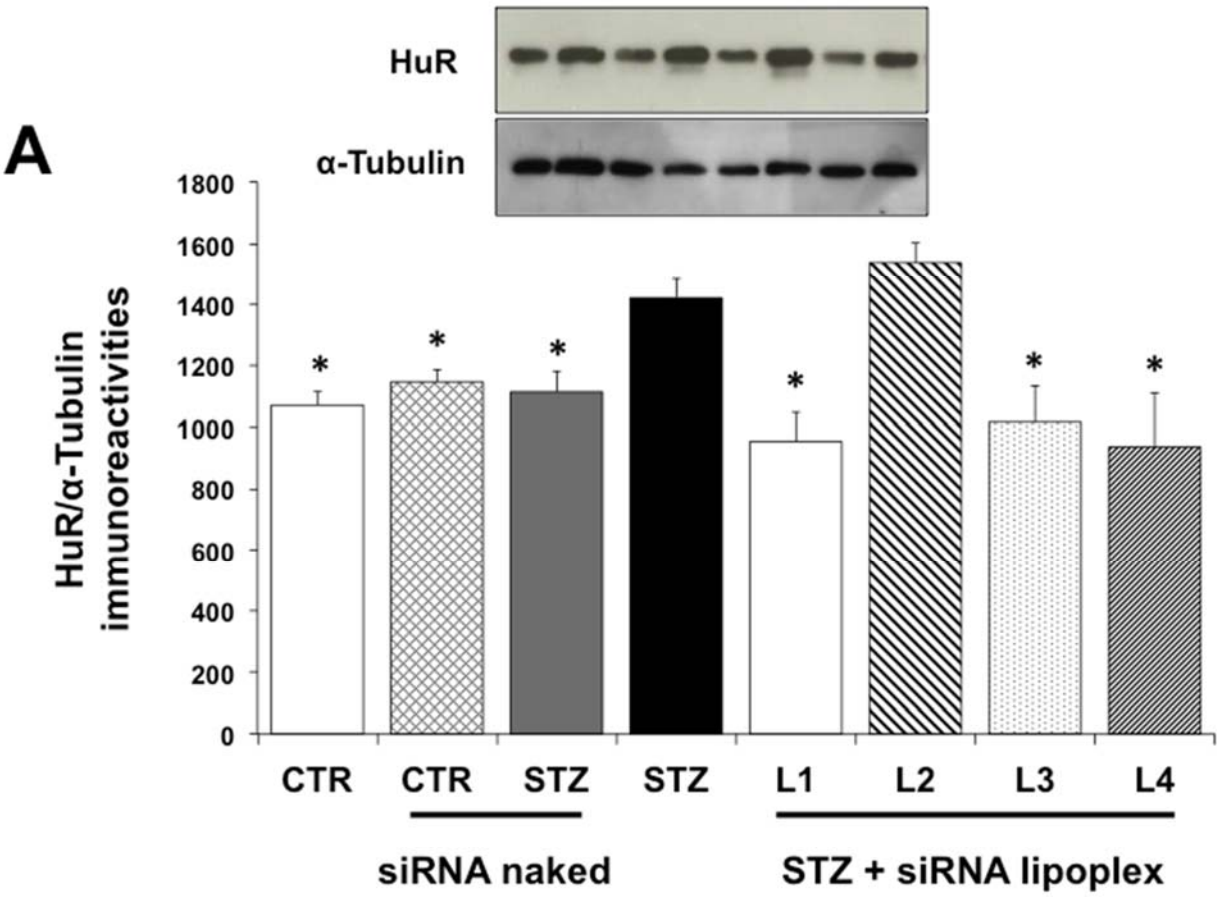
A
HuR
α-Tubulin
HuR/α-Tubulin immunoreactivities
1800
1600
1400
1200
1000
800
600
400
200
0
CTR
CTR
STZ
STZ
L1
L2
L3
L4
siRNA naked
STZ + siRNA lipoplex

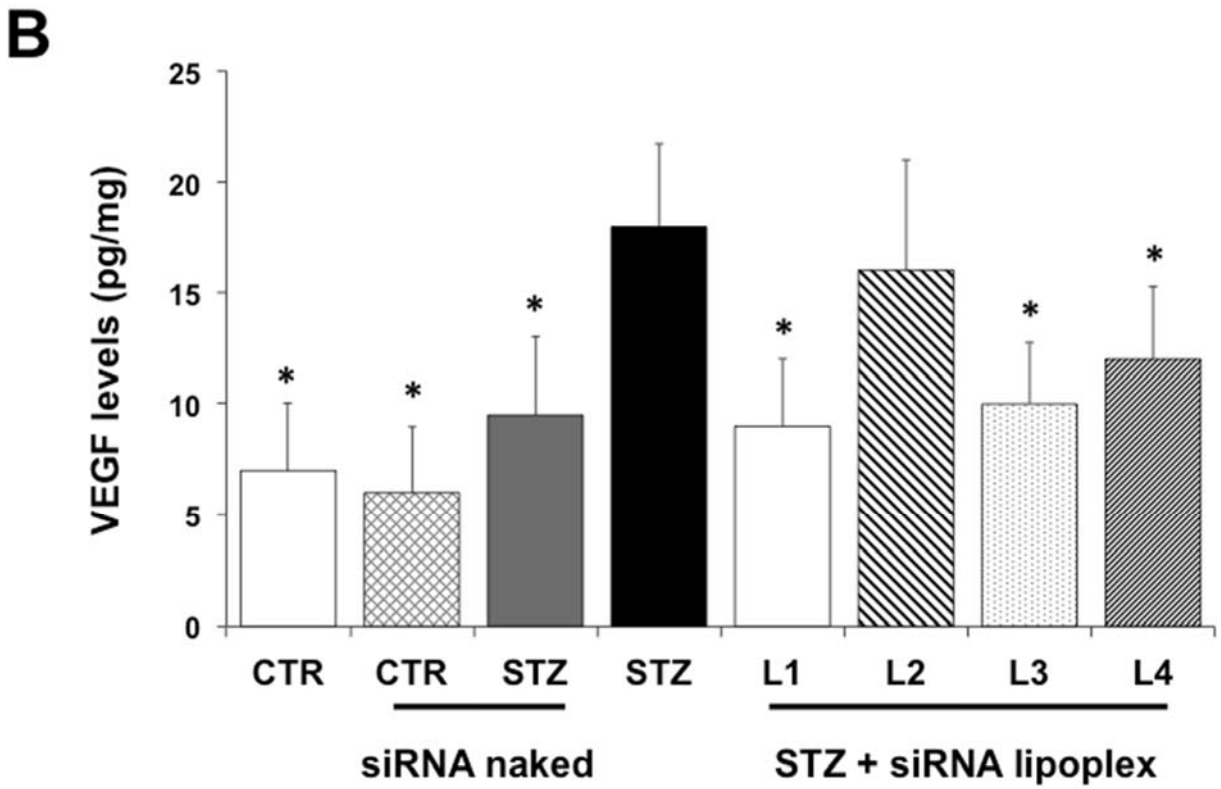
B
VEGF levels (pg/mg)
25
20
15
10
5
0
CTR
CTR
STZ
STZ
L1
L2
L3
L4
siRNA naked
STZ + siRNA lipoplex

Fig. 3. Effects of intraocular injection of lipid nanocarriers carrying HuR siRNA. (Panel A) Representative Western blotting gels (upper) and mean grey level ratios of HuR/α-tubulin immunoreactivities (lower) in the retina of animal receiving vehicle (for STZ group), siRNA naked or in nanocarriers (siRNA lipoplex; L1-L4). *$p<0.05$ *vs.* STZ. Tukey multiple comparisons test, n=7–12; (Panel B) Retinal levels of VEGF (pg/mg, ±S.D.) measured by ELISA. * $p<0.05$ *vs.* STZ. Dunnett's test, n=5–8.

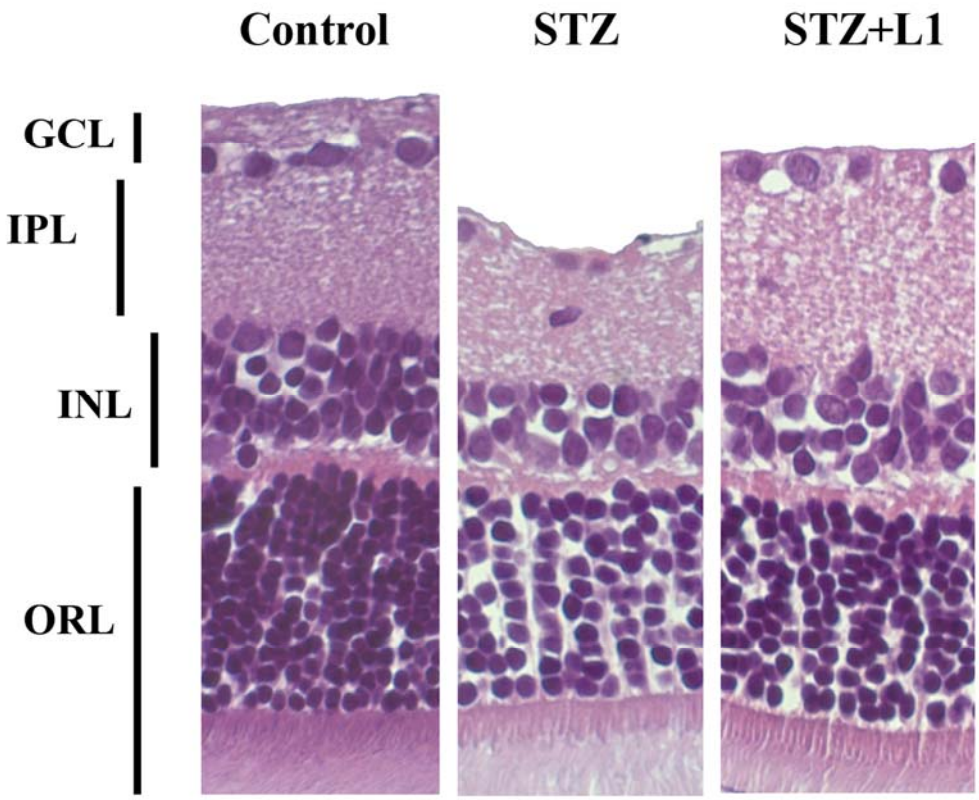

Fig. 4. Representative micrographs of rat retina obtained from control group (normal rats), STZ group (rats with diabetes) and STZ + L1 (diabetic rats treated with HuR siRNA lipoplex L1). Images show paraffin-embedded retina sections stained with hematoxylin–eosin. Micrographs are representative results taken from different fields of randomly selected slides and photographed at 40× magnification under a light microscope. Retinal layers are indicated, on the left part of the figure, as follows: GCL, ganglion cell layer; IPL, inner plexiform layer; INL, inner nuclear layer; ORL, outer retinal layer.

References

1. R.A. Brook, N.L. Kleinman, S. Patel, J.E. Smeeding, I.A. Beren, A. Turpcu, United States comparative costs and absenteeism of diabetic ophthalmic conditions, Postgrad. Med. 31 (2014) 1-8.
2. S.J. Song, T.Y. Wong, Current concepts in diabetic retinopathy, Diabetes Metab. J. 38 (2014) 416-425.
3. M.W. Stewart, Anti-vascular endothelial growth factor drug treatment of diabetic macular edema: the evolution continues, Curr. Diabetes Rev. 8 (2012) 237-46.
4. A.W. Stitt, N. Lois, R.J. Medina, P. Adamson, T.M. Curtis, Advances in our understanding of diabetic retinopathy. Clin. Sci. (Lond) 1251 (2013) 1-17.

5. A.P. Levy, N.S. Levy, M.A. M.A., Goldberg, Post-transcriptional regulation of vascular endothelial growth factor by hypoxia, J. Biol. Chem. 271 (1996) 2746-2753.

6. N.S. Levy, S. Chung, H. Furneaux, A.P. Levy, Hypoxic stabilization of vascular endothelial growth factor mRNA by the RNA-binding protein HuR, J. Biol. Chem. 273 (1998) 6417-6423.

7. C. Osera, J.L. Martindale, M. Amadio, J. Kim, X. Yang, C. A. Moad, F.E. Indig, S. Govoni, K. Abdelmohsen, M. Gorospe, A. Pascale, Induction of VEGFA mRNA translation by $CoCl_2$ mediated by HuR, RNA Biol. 1 (2015) 1-10.

8. L.B. Nabors, G.Y. Gillespie, L. Harkins, P.H. King, HuR, a RNA stability factor, is expressed in malignant brain tumors and binds to adenine- and uridine-rich elements within the 3' untranslated regions of cytokine and angiogenic factor mRNAs, Cancer Res. 61 (2001) 2154-2161.

9. M. Amadio, G. Scapagnini, U. Laforenza, M. Intrieri, L. Romeo, S. Govoni, A. Pascale, Post-transcriptional regulation of HSP70 expression following oxidative stress in SH-SY5Y cells: the potential involvement of the RNA-binding protein HuR, Curr. Pharm. Des. 14 (2008) 2651-2658.

10. Z. Yuan, A.J. Sanders, L. Ye, W.G. Jiang, HuR, a key post-transcriptional regulator, and its implication in progression of breast cancer, Histol. Histopathol. 25 (2010) 1331-1340.

11. P. Milani, M. Amadio, U. Laforenza, M. Dell'Orco, L. Diamanti, V. Sardone, S. Gagliardi, S. Govoni, M. Ceroni, A. Pascale, C. Cereda, Posttranscriptional regulation of SOD1 gene expression under oxidative stress: Potential role of ELAV proteins in sporadic ALS, Neurobiol. Dis. 60 (2013) 51-60.

12. M. Amadio, G. Scapagnini, S. Davinelli, V. Calabrese, S. Govoni, A. Pascale, Involvement of ELAV RNA-binding proteins in the post-transcriptional regulation of HO-1, Front. Cell. Neurosci. 15 (2015) 459.

13. M. Amadio, C. Bucolo, G.M. Leggio, F. Drago, S. Govoni, A. Pascale, The PKCbeta/HuR/VEGF pathway in diabetic retinopathy, Biochem. Pharmacol. 80 (2010) 1230-1237.

14. C. Bucolo, G.M. Leggio, F. Drago, S. Salomone. Eriodictyol prevents early retinal and plasma abnormalities in streptozotocin-induced diabetic rats, Biochem. Pharmacol. 84 (2012) 88-92.

15. J.E. Podesta, K. Kostarelos, Engineering cationic liposome: siRNA complexes for in vitro and in vivo delivery, in: Nejat Düzgüneş (Ed.), Methods in Enzymology, Academic Press, Burlington, 2009, pp. 343-354.

16. R. Pignatello, C. Bucolo, G. Spedalieri, A. Maltese, G. Puglisi, Flurbiprofen-loaded acrylate polymer nanosuspensions for ophthalmic application, Biomaterials 23 (2002) 3247-3255.

17. R. Pignatello, A. Leonardi, S. Cupri, Optimization and validation of a new method for the production of lipid nanoparticles for ophthalmic application, Int. J. Med. Nano Res. 1 (2014) 11.

18. J. Kusari, S. Zhou, E. Padillo, K.G. Clarke, D.W. Gil, Effect of memantine on neuroretinal function and retinal vascular changes of streptozotocin-induced diabetic rats, Invest. Ophthalmol. Vis. Sci. 48 (2007) 5152-5159.

19. S. Scuderi, A.G. D'Amico, C. Federico, S. Saccone, G. Magro, C. Bucolo, F. Drago, V. D'Agata, different retinal expression patterns of IL-1α, IL-1β, and their receptors in a rat model of type 1 STZ-Induced diabetes, J Mol Neurosci. 56 (2015) 431-439.

20. D. Belletti, M. A. Vandelli, M. Tonelli, M. Zapparoli, F. Forni, G. Tosi, B. Ruozi, Functionalization of liposomes: microscopical methods for preformulative screening, J. Liposome Res. 25 (2015) 150–156.

21. X. Shi, S. Liao, H. Mi, C. Guo, D. Qi, F. Li, C. Zhang, Z. Yang, Hesperidin prevents retinal and plasma abnormalities in streptozotocin-induced diabetic rats, Molecules. 17 (2012) 12868-12881.

22. J.W. Park, S.J. Park, S.H. Park, K.Y. Kim, J.W. Chung, M-H. Chun, S.J. Oh, Up-regulated expression of neuronal nitric oxide synthase in experimental diabetic retina, Neurobiol. Dis. 21 (2006) 43-49.

23. S.A. Tenenbaum, P.J. Lager, C.C. Carson, J.D. Keene, Ribonomics: identifying mRNA subsets in mRNP complexes using antibodies to RNA-binding proteins and genomic arrays, Methods 26 (2002) 191-198.

24. D. Antic, J.D. Keene, Messenger ribonucleoprotein complexes containing human ELAV proteins: interactions with cytoskeleton and translational apparatus, J. Cell Sci. 111 (1998) 183-197.

25. R. Hovland, J.E. Hesketh, I.F. Pryme, The compartmentalization of protein synthesis: importance of cytoskeleton and role in mRNA targeting. Int. J. Biochem. Cell Biol. 28 (1996) 1089-1105.

26. M. Amadio, G. Scapagnini, G. Lupo, F. Drago, S. Govoni, A. Pascale, PKCbetaII/HuR/VEGF: A new molecular cascade in retinal pericytes for the regulation of VEGF gene expression, Pharmacol. Res. 57 (2008) 60-66.

27. M. Amadio, C. Osera, G. Lupo, C. Motta, F. Drago, S. Govoni, A. Pascale, Protein kinase C activation affects, via the mRNA-binding Hu-antigen R/ELAV protein, vascular endothelial growth factor expression in a pericytic/endothelial coculture model, Mol. Vis. 18 (2012) 2153-2164.

28. M. Amadio, S. Govoni, A. Pascale, Targeting VEGF in eye neovascularization: what's new? a comprehensive review on current therapies and oligonucleotide-based interventions under development, Pharmacol. Res. 103 (2015) 253-269.

29. S. Chen, J. Feng, L. Ma, Z. Liu, W. Yuan, RNA interference technology for anti-VEGF treatment, Expert Opin. Drug Deliv. 11 (2014) 1471-1480.